JOURNAL OF GEOPHYSICAL RESEARCH, VOL. 104, NO. A8, PAGES 17,069–17,078, AUGUST 1, 1999

Langmuir waves in a fluctuating solar wind

P. J. Kellogg,[1] K. Goetz, and S. J. Monson
School of Physics and Astronomy, University of Minnesota, Minneapolis

S. D. Bale
Space Sciences Laboratory, University of California, Berkeley

Abstract. The Langmuir waves which are resonant with typical type III solar radio burst electrons have a frequency so little above the ambient plasma frequency that they should be strongly affected by known density fluctuations. Some consequences of this observation are worked out, and the expected consequences are demonstrated in the observations of the Langmuir waves from two quite different bursts, of November 4, 1997, and January 19, 1998.

1. Introduction

As pointed out in an earlier paper [*Kellogg*, 1986], the resonant Langmuir waves created by the electrons of a typical type III solar burst, energy of order 2-10 keV, lie very close to the local plasma frequency. For typical solar wind parameters, i.e., $T_e = 10$ eV, the resonant frequency is 1.0037 f_{pe} at $kc/\omega_p = 11.3$ for a 2 keV beam, and 1.00074 f_{pe} at $kc/\omega_p = 5$ for a 10 keV beam. These are obtained from the resonance condition,

$$\omega = kv_b \tag{1}$$

and the Bohm-Gross dispersion relation,

$$\omega^2 = \omega_p^2 + 3k^2k_BT/m \tag{2}$$

Observed density fluctuations imply variations of the plasma frequency which are larger than these differences, so that these fluctuations must play an important role in the generation of type III bursts. For Langmuir waves in the Earth's electron foreshock the situation is essentially similar, though it is likely that the electron beams are slower and that the waves are created at a somewhat higher frequency. *Kraus-Varban* [1989] explored the theoretical consequences of these properties. *Bale et al.* [1998] have presented observations lending support.

In this work, we report some observations made with the Waves experiment [*Bougeret et al.*, 1995] on the Wind satellite and some further analysis, which lend additional support to these considerations. Most of the results will come from the Time Domain Sampler (TDS), which makes rapid samples of the potential difference between the two halves of dipole antennas and which was designed to investigate the interactions of Langmuir waves. We present results from two type III bursts which passed over Wind and which resulted in a fairly large number of events appropriate for more detailed analysis.

2. Density Fluctuations, the WKB Approximation, and Mode Evolution

In Figure 1 some synthetic density data calculated from published density power spectra are shown [*Unti et al.*, 1973; *Neugebauer*, 1975, 1976; *Celniker et al.*, 1983, 1987]. To make these curves, which essentially means reconstructing a time series statistically similar to the original data from which the power spectra were calculated, we have calculated a Fourier series for a much longer time period than shown (100 times longer), in which each amplitude is proportional to the square root of the power spectrum, integrated over the increment in frequency appropriate to a harmonic coefficient of the longer time period, and we have given the Fourier amplitude a random phase between 0 and 2π and then done an inverse transform. The data used in Figure 1 were from *Neugebauer* [1976], but the other measurements are consistent, within the large fluctuations, except at frequencies above 1 Hz. Then we calculate a short time section of the sum of this Fourier series, which gives the fractional density fluctuations shown in Figure 1. For a typical plasma density of 7 cm^{-3} this implies relative variations in the local plasma frequency, which are shown on the axis to the right and which are larger than the difference between the resonant frequency above and the plasma frequency. Rather than weak scattering treated as a perturbation, the relevant regime is then complete reflection or partial reflection and tunneling, linear mode conversion, etc.

However, the spectrum used to construct the density fluctuations of Figure 1 is an average of a large number of individual spectra with fluctuation power differing by a large factor. We have taken

$$P = 5 \times 10^{-3} f^{-1.54} \tag{3}$$

for frequency less than 1 Hz and zero above, where P is spectral power in cm^{-6} Hz^{-1}. Hence one might expect some periods

[1] Formerly at Observatoire de Paris, Meudon, France.

Copyright 1999 by the American Geophysical Union.

Paper number 1999JA900163.
0148-0227/99/1999JA900163$09.00

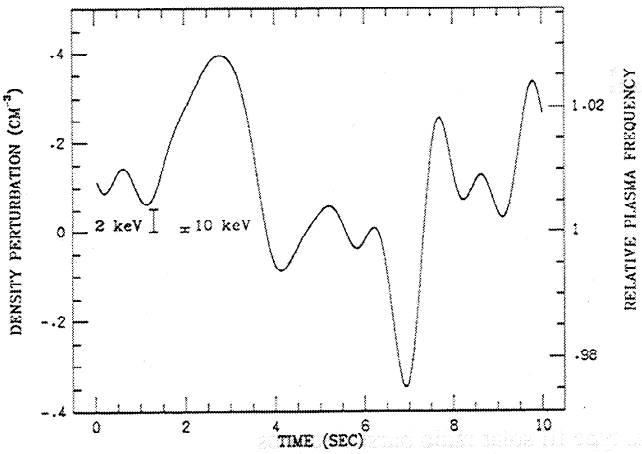

Figure 1. A time series of density fluctuations reconstructed from an averaged spectrum [*Neugebauer*, 1976]. The two brackets at the left show the difference between the plasma frequency and the resonant frequency for electron beams of 2 and 10 keV.

when the density fluctuations are reduced and the trapping is not as extreme as that in Figure 1 and also more extreme cases.

It is believed that the spectrum of density fluctuations decreases rapidly for frequencies above about 1 Hz [*Neugebauer*, 1975, 1976; *Kellogg and Lin*, 1997]. Therefore, as a Langmuir wave propagates through the varying density medium, its frequency will remain approximately constant, since it sees a medium whose time variations are nearly zero. The accuracy of this assumption will be discussed below. If the spatial variations are sufficiently slow that the WKB approximation holds, then the wave number will change to satisfy the dispersion relation. A particularly interesting case is when the wave approaches a density increase. In Figure 2 some calculations relevant to this case are shown. The left section shows the traditional dispersion diagram for a weakly magnetized plasma like the solar wind, and the right section shows a detail for small k. We suppose that initially a wave was generated at an appropriate place on the curves of the left section as calculated above but that the plasma frequency has increased along the path of the wave, so that it finds itself even closer to the plasma frequency and in the region shown in the right section. In Figure 2 (right), the top section shows, as a solid line, the solutions of the dispersion relation for the three relevant waves, i.e., the left- and right-hand polarized waves and the longitudinal wave, in the vicinity of the plasma frequency.

The full description of these waves requires an augmentation of the usual Stokes parameters to take into account the longitudinal components of the waves, which do not exist in vacuum. Since these are theoretical calculations, those Stokes parameters which describe the orientation of the principal polarization axis with respect to the observing system are not useful, nor is the first Stokes parameter, which is the intensity of the wave. In the conventional coordinate system in plasma physics the ambient magnetic field lies in the z direction, and the wave vector $\mathbf{k}$ lies in the x-z plane. For the augmented Stokes parameter system we chose axes parallel to $\mathbf{y} \times \mathbf{k}$, $\mathbf{y}$, and $\mathbf{k}$. In the lower two sections of Figure 2 (right) we have shown Q, which is a usual Stokes parameter,

$$Q = \frac{E_{y\times k}^2 - E_y^2}{E_{y\times k}^2 + E_y^2} \tag{4}$$

and an augmentation of the Stokes parameters, the ratio of the longitudinal component of E to the total, using squares or intensities in keeping with the spirit of the original Stokes parameters,

$$R_{LEm} = \frac{E_k^2}{E_k^2 + E_y^2 + E_{y\times k}^2} \tag{5}$$

Value Q, which shows the degree of circular polarization of the transverse components, is the difference of the squares of the two transverse components of E divided by their sum. A value of $Q = 0$ means circular polarization, $Q = -1$ means linear polarization in the $\mathbf{y}$ direction, and $Q = +1$ means linear polarization in the $\mathbf{y} \times \mathbf{k}$ direction. The lowest section in Figure 2 (right) shows R_{LEm}, the ratio of the square of the longitudinal field to the square of the total. The phases are not shown, but the $\mathbf{y}$ component is 90° out of phase with the longitudinal component, while the $\mathbf{y} \times \mathbf{k}$ component is in phase with it. As a wave moves into a density increase and to the left along the dispersion curve, it begins to acquire some transverse electric field components. In this region the wave mode is called the Z mode. It is the y component which increases more rapidly at first, so that the electric vector traces out an ellipse, which, however, lies in the plane of the wave vector $\mathbf{k}$, not perpendicular to it as one usually expects for elliptical polarization. At still smaller $\mathbf{k}$ the $\mathbf{y} \times \mathbf{k}$ component, which is in phase with the longitudinal component, becomes appreciable, so that the electric vector is no longer along $\mathbf{k}$, and the ellipse begins to tip toward the plane perpendicular to $\mathbf{k}$.

The magnitude of $\mathbf{k}$ cannot generally be measured for the long-wavelength resonant waves which result from (1) and (2), still less for those of an approach of a Langmuir wave to a density increase. In this work, we look for circular polarization or a transverse component to provide the clue that the Langmuir wave is becoming Z mode.

However, the WKB approximation is not valid for the conditions shown in Figure 2 (right) because the wavelength becomes so long. Typical density changes in Figure 1 are of order $10^{-1}\mathrm{cm}^{-3}\,\mathrm{s}^{-1}$, or

$$\frac{dn}{dx} \approx \frac{1}{v_{sw}}\frac{dn}{dt} \approx 3\ 10^{-9}\mathrm{cm}^{-4} \tag{6}$$

for a solar wind speed of 325 km s^{-1} as on November 4. The condition that the WKB approximation be valid is that the change of wavelength in one wavelength be small compared to a wavelength:

$$\frac{1}{\lambda}\left(\frac{d\lambda}{dx}\lambda\right) = \frac{d}{dx}\left(\frac{2\pi}{k}\right) = \frac{2\pi}{k^2}\frac{dk}{d\omega_p}\frac{d\omega_p}{dx} << 1 \tag{7}$$

where it is assumed that the frequency remains constant. From

$$\omega \approx \omega_p + \frac{3}{2}\frac{k^2 v_{te}^2}{\omega_p} \tag{8}$$

with $v_{te}^2 = k_B T / m$, we have, neglecting a small term,

$$\frac{\mathrm{dk}}{\mathrm{d}\omega_\mathrm{p}} = -\frac{1}{3}\frac{\omega_\mathrm{p}}{\mathrm{k}v_{\mathrm{te}}^2} \tag{9}$$

The WKB approximation is then valid for

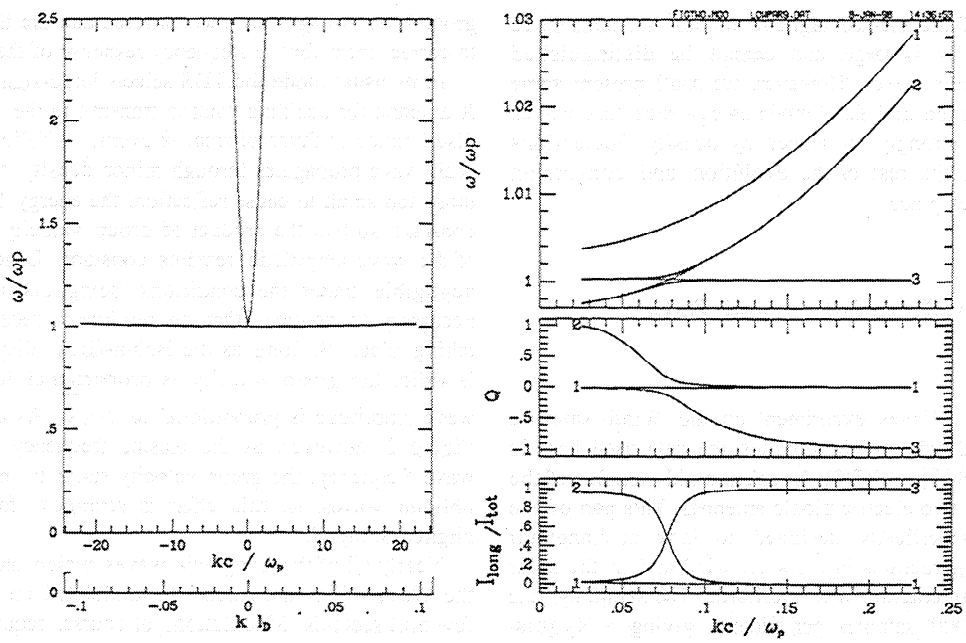

Figure 2. (left) Diagram of ω versus k for a weakly magnetized solar wind. The electromagnetic modes, for which f/f_p becomes large, cannot be distinguished on this scale. (right) A detail near the origin of 2*a*. The dotted line shows the dispersion relation for propagation parallel to B, and the solid line shows the dispersion relation for propagation at an angle of 11°. The curves marked 1 and 2 are the ordinary and extraordinary electromagnetic modes, respectively; curve 3 is the Langmuir mode. The lower two sections show Q, the Stokes parameter, and R_{LEm}, the ratio of the longitudinal intensity to the total intensity. These results are from a warm magnetized plasma code.

$$\frac{\pi}{3}\left(\frac{\omega}{kc}\right)^3 \frac{c^2}{v_{te}^2}\frac{c}{\omega_p}\left(\frac{1}{n}\frac{dn}{dx}\right) << 1 \qquad (10)$$

For a solar wind speed of 325 km s^{-1}, T_e = 10 eV, and f_p = 27 kHz, as on November 4, we have

$$k c/\omega_p >> 3 \qquad (11)$$

The limit is just the region of interest for type III bursts. The breakdown of the WKB approximation due to spatial variations of density means that k is no longer a constant of the motion, so parts of Figure 2 (right) at different k but at the same ω will be mixed together. We may therefore expect transverse components of waves to k values well beyond those shown in Figure 2 (right) to the limit where the WKB approximation starts to be valid.

Of course, the medium is also time varying, but slowly. Mixing different ωs may be expected over a range of kv_s, where v_s is the speed of the constant density surfaces. We expect that this is the Alfven speed or the ion sound speed or less, and these are of the order of 50 km s^{-1}, giving for kc/ω_p = 3 and f_p = 27 kHz again,

$$\frac{\Delta f}{f_p} = \frac{kv_s}{\omega_p} = 7\times10^{-4} \qquad (12)$$

to give Δf = 20 Hz, which would cause mixing across the small gap in Figure 2 (right) to the O mode but which would be expected to cause less mixing to the other electromagnetic mode, separated by $f_c/2$ = 80 Hz, where f_c is the electron cyclotron frequency.

As a resume of these considerations, we show below a list of important values of kc/ω_p. To the values discussed above, we have added the critical value for three-wave parametric decay, Langmuir wave to Langmuir wave plus ion sound wave, as that will be important in section 3 [*Akhiezer et al.*, 1975]:

resonant with 2 keV beam	kc/ω_p = 11.3
resonant with 10 keV beam	kc/ω_p = 5.0
WKB approximation valid	kc/ω_p >> 3.0 (6 is OK)
three-wave decay $L \rightarrow L' + S$	kc/ω_p = 7.0

In summary, to the extent that the WKB approximation is valid and the frequency is constant, we should expect a conversion of the Langmuir waves to Z mode as a density increase is approached. Breakdown of the WKB approximation and breakdown of the assumption of constant frequency may happen very close to the critical density where the wave frequency is equal to one of the cutoff frequencies, and there we should expect mixing and conversion of one mode to another. It is clear that a treatment of the full set of differential equations is necessary. Recently, *Yin et al.* [1998] have made calculations of reflection and mode coupling in an initial foray into a proper solution of the problem. Their results do not differ grossly from the results of an earlier analytic calculation which neglected magnetic fields [*Hinkel-Lipsker et al.*, 1992]. The results of both calculations are that there is a narrow range of angles in which conversion to electromagnetic modes has an efficiency of the order of 50%, and so type III electromagnetic bursts may be efficiently generated by mode conversion of Langmuir waves. The data which are available to us do not allow a complete verification of this whole sequence of wave evolution in density fluctuations. In particular, the electric

field amplitude of the electromagnetic modes is small, since their group velocity is large, and cannot be distinguished against the Langmuir waves. However, we shall present some evidence for reflection and for Z mode as evidence that waves are actually being strongly influenced by density fluctuations and therefore that the rest of the evolution and conversion probably also takes place.

3. Experiment Description and Data Treatment

The part of the Waves experiment on the Wind satellite [*Bougeret et al.*, 1995] which provides the data used here is the Time Domain Sampler (TDS). It makes rapid samples of the waveform seen on two electric dipole antennas. This part of the experiment was specifically designed to look at Langmuir waves and their interactions in the solar wind and in the solar wind's region of interaction with the Earth. The sampling rate used here is 120,000 samples per second, giving a Nyquist frequency of 60 kHz. At this sampling rate, the data from only two of the three electric dipole antennas can be sent to earth. Most often, the X and Y antennas, in the spin plane and also in the GSE *x-y* plane, are used. Hence the results presented here are projections of the electric fields in the GSE *x-y* plane. The X antenna is a 100 m tip-to-tip dipole, and the Y is a 15 m tip-to-tip dipole. In order to provide a larger dynamic range, the voltages are compressed logarithmically, on board. On the ground the voltages are reconstituted and are Fourier analyzed to correct them for the frequency response of the system.

In its usual mode the TDS selects large-signal events on the X antenna for deciding what to transmit to the Earth. This will discriminate in favor of small-k events as follows: As a Langmuir wave propagates through minor density fluctuations, i.e., those too small to cause reflection, the energy flux must remain constant, so that the product of group velocity and the square of the wave amplitude remains constant. Landau damping is negligible under the conditions being discussed, but it is necessary to assume that no nonlinear decay processes are taking place. So long as the Bohm-Gross dispersion relation is valid, the group velocity is proportional to k, so that the wave amplitude is proportional to $1/\sqrt{k}$. As can be seen from Figure 2, however, as the plasma frequency approaches the wave frequency, the group velocity starts to increase again for oblique waves, so this effect is strongest for waves nearly aligned along B.

Nearly all of the Langmuir waves which are observed with the Waves TDS instrument are modulated on a timescale of a few milliseconds. Modulation, of course, requires a mixture of waves. This mixture could be due to (1) a spectrum of waves which have nearly the same wave vectors, such as would be produced by an instability which has an unstable region of finite size, (2) a three-wave decay process which produces a daughter wave of appreciable amplitude, (3) partial or complete reflection of a wave, for example, by a density jump, (4) variation of wave number due to variations of the plasma parameters, or (5) the wave growing or decaying rapidly due to

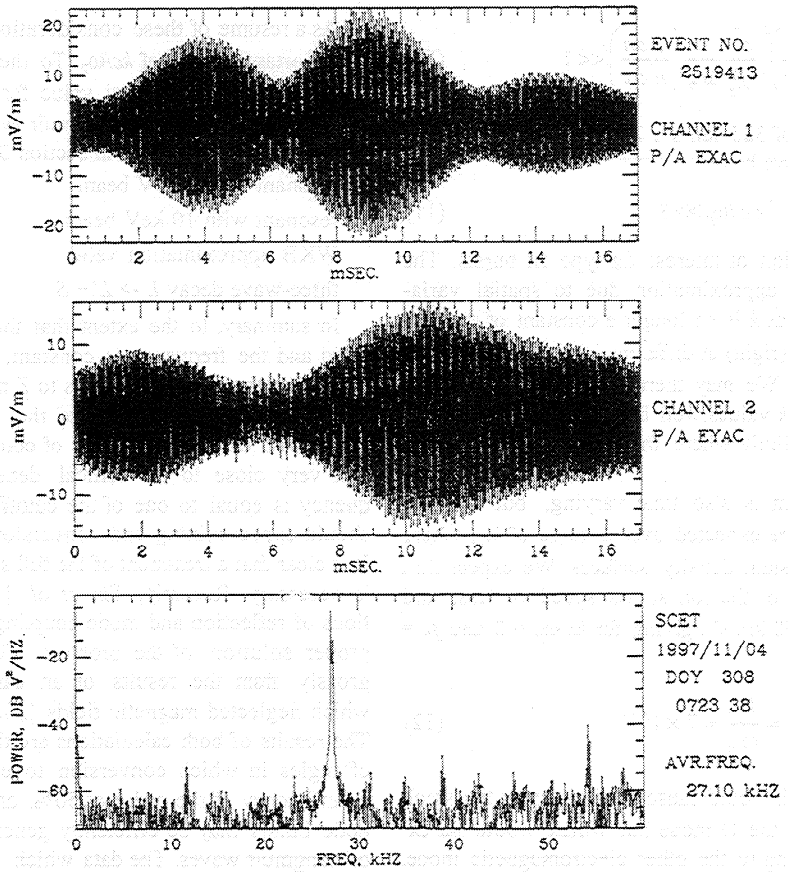

Figure 3. Comparison of the simultaneous signals on two orthogonal antennas. In Figures 3 and 4 it can be seen that there must be at least two waves, at appreciable angles to each other.

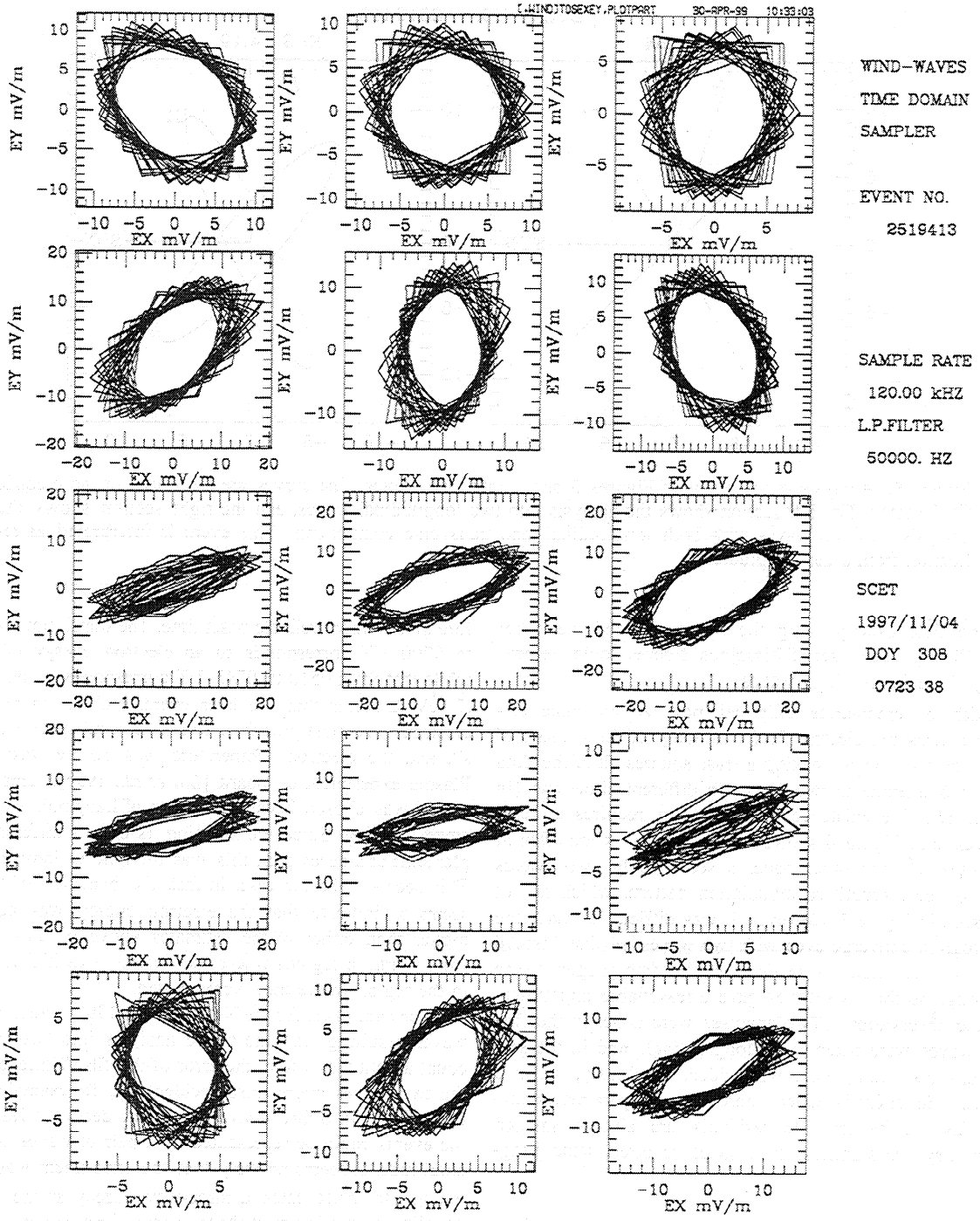

Figure 4. Lissajous figures, i.e., EY versus EX, for the event of Figure 3. If the experiment were sampling a longitudinal wave, the figures would just be straight lines.

an instability in progress or to damping. Probably most of these effects occur, and they are hard to separate.

In many cases, the waveform seen on the X antenna is different from the waveform seen on the Y antenna. An example chosen to illustrate this is shown in Figure 3. If the wave packet consisted of a spectrum of nearly colinear longitudinal waves, the two waveforms would be nearly identical in shape and would differ only in amplitude because of the angles between the wave vector and the antennas. The observed difference can then only be due to waves with wave vectors in significantly different directions. This argues against the interpretation of the observed modulation as being due to a spectrum of growing waves, i.e., to a wave packet for which all the wave vectors belong to the narrow region in k space for which growth is strong.

For the event of Figure 3 we have divided the event into 15 equal parts, and in Figure 4 we have plotted EY, the signal on the Y antenna, versus EX, to make a series of figures. The time sequence begins at the lower left and proceeds across. While some sections suggest elliptical polarization, Figure 4 does not unequivocally demonstrate it. To see this, consider two longitudinal waves of slightly different frequency, one with

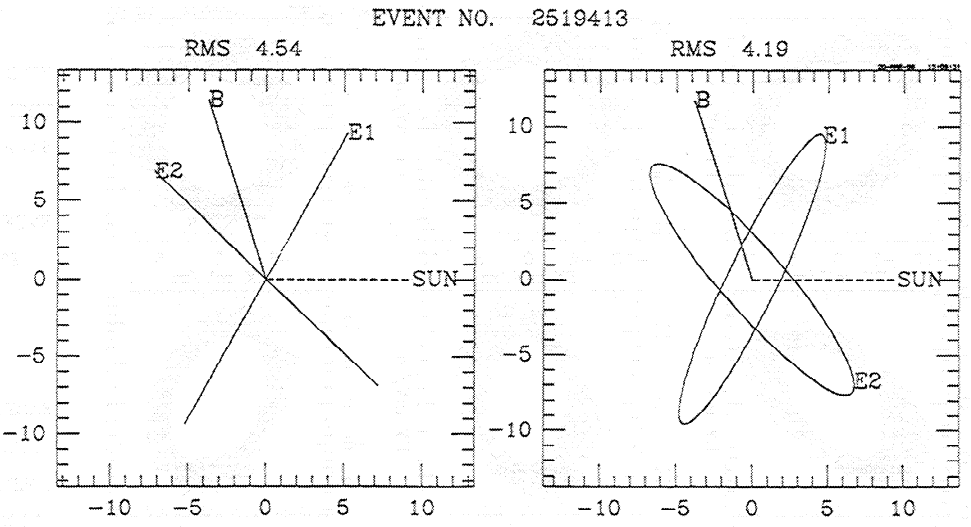

Figure 5. Analysis of the event of Figures 3 and 4 into two waves. The curves are the traces of the electric field vector. The left section shows the analysis into two longitudinal waves, and the right section shows the analysis into two waves with both longitudinal and transverse components. This event is interpreted as reflection from a density gradient.

its electric field exactly along the X antenna and the other along Y. Clearly, such a set of Lissajous figures could be produced by these longitudinal waves.

In order to demonstrate elliptical polarization more certainly, the measured electric field was analyzed into a sum of the fields of two waves, making a least squares fit of the data from the two antennas to two waves in different directions (in the *x-y* plane). The existence of modulation requires at least two waves, and Figure 4 shows that these waves are often at large angles. On the other hand, a set of only two waves would produce a repetitive modulation pattern, which is not what is seen in Figure 3. However, it was difficult to make the fitting program converge even with two waves, so that instead the program was used on sections of the data judged to be short enough so that two waves gave a reasonable approximation to the observations. Two analyses were done. In the first the two waves were taken to be longitudinal, and in the second a transverse component was added. Obviously, when a transverse component is added, there are more parameters, and so the fits are better: The residuals are always smaller. Whether they are significantly smaller requires some judgment.

4. Observations: November 4, 1997

To apply these considerations to measurements, we have first chosen some data from the Langmuir waves generated by a type III burst on November 4, 1997. There were two large type III bursts beginning at 0510 and 0555 (times are UT hours and minutes at the spacecraft) as seen by the radio part of the Waves experiment. The first Langmuir waves captured by the TDS were at 0715 UT, and a total of 16 events were captured and telemetered over the period 0715–0743 UT, with one more weak Langmuir wave event at 0802 UT. However, another part of the Waves experiment, the Thermal Noise Receiver (TNR), saw the first Langmuir waves at 0700 UT. This is not unusual as the TDS selects only the largest events, and the TNR therefore gives a more reliable onset time. The transit time from 0555 to 0700 UT corresponds to an electron energy of 4.5 keV, while that from 0510 to 0743 UT corresponds to an energy of .7 keV. It seems that the later event, and the more energetic electrons, are most probable. The solar wind speed was 325 km s^{-1}, and the electron temperature was 10 eV, from the 3-D Plasma experiment on board [*Lin et al.*, 1995]. This series of events was chosen because the sets of Langmuir waves show small splitting. Since the splitting is often a differential Doppler shift of a decay pair, this was thought to indicate small k. This seems to be the case. In fact, the behavior of the waves seems to indicate that the electron energy was appreciably higher than either of the estimates above or that the waves were found in regions where the density was higher than that in the region where they were created.

In several cases for the November 4, 1997, event the pair of waves resulting from the above analysis into two waves had equal amplitudes within the error of the fits. While equality of the two waves might arise accidentally, for example, at a certain instant in a three-wave parametric decay, at least three of the events could be represented by a pair of waves of the same amplitude. It seems unlikely that the experiment was fortunate enough to thrice catch a three-wave decay at the moment of equality, so we interpret these events as reflection.

In Figure 5 the two-wave analysis for the event of Figure 3 is shown. What is shown is the projection of one cycle of the electric field vector on the *x-y* plane. The left section shows the analysis into two longitudinal waves, and the right section shows an added transverse component. The arrows give the directions of rotation. The rms residuals of the fits, in mV m^{-1}, are shown at the top of the graphs. The lines or ellipses marked E1 are for the wave with the lower observed frequency, though we interpret the frequency difference as due to Doppler shift. Since the medium is not isotropic, reflection is not necessarily specular. In this example it can be seen that the wave is reflected at a plane which is either parallel or perpendicular to B, so that the angle of reflections should be equal to the angle of incidence, and the waves should have the same longitudinal and (possibly) transverse components.

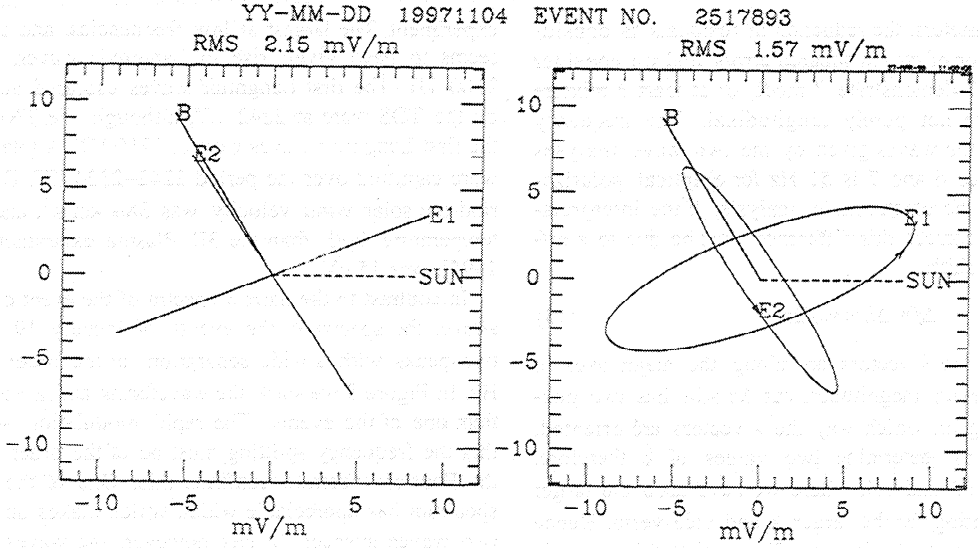

Figure 6. An analysis like that of Figure 5 for another event, where the reflection causes some change of wave properties. Arrows show the directions of rotation.

Another case which appears to be reflection but is not specular reflection, is shown in Figures 6 and 7. Again, the waveform does not repeat well, and analysis of the second half of the event only is shown in Figure 6. In this case one wave is nearly longitudinal and along B. The other wave is nearly perpendicular to B. It will be seen that the wave which is propagating nearly perpendicular to B has an appreciably larger transverse component, as expected. In both cases it will be seen that the longitudinal wave analysis is doing its best to represent the waves but that the residuals from the elliptical polarization fit are appreciable smaller. Although the residuals from the transverse analysis must necessarily be smaller since

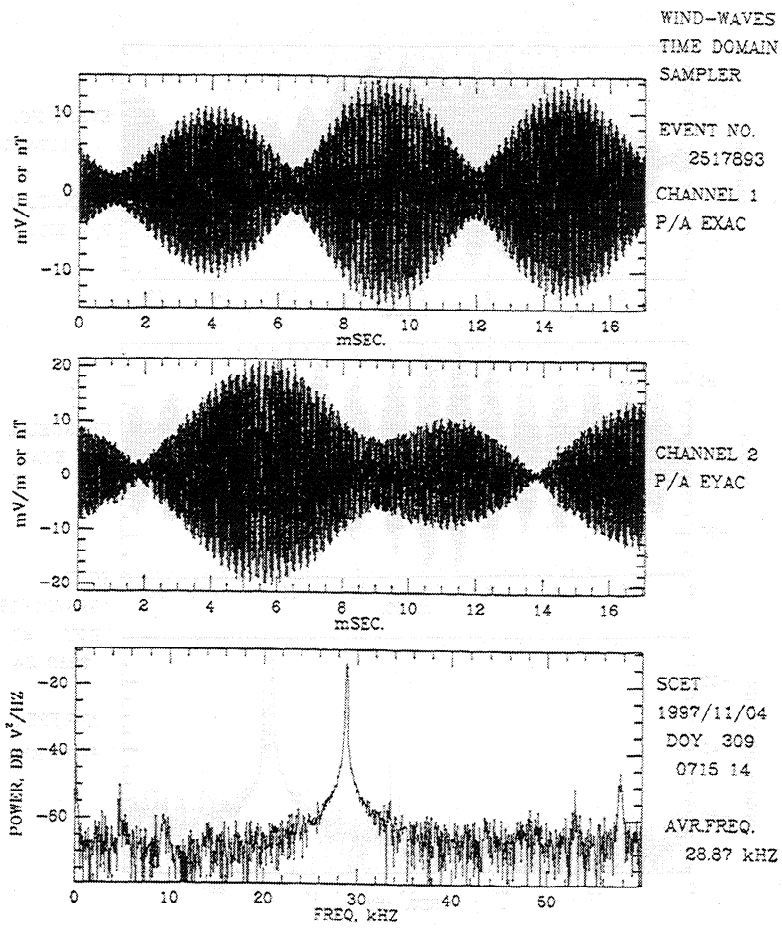

Figure 7. The simultaneously sampled signals on two antennas for the event of Figure 6.

there are more parameters, the reduction in residuals is considerable, nearly a factor of two in squared errors, and we consider that Figures 6 and 7 demonstrate Z mode, or at least a mixture of modes which are not purely longitudinal. The frequency difference between the waves given by the two wave analyses of the data in Figures 6 and 7 is 51 Hz for elliptical polarization and 44 Hz for the electrostatic analysis. If the interpretation of reflection is correct, this difference must be due to a difference in Doppler shift:

$$\Delta f = \Delta k \times v_{sw}/2\pi \tag{13}$$

We assume that the k vectors are along the major axes in Figure 6 and have equal magnitudes, but Δk still has two possibilities, depending on which way the k vectors are oriented. These considerations determine two values of k, therefore, which are $kc/\omega_p = 4.5$ and 1.4, where we have used the larger value of 51 Hz splitting for the larger k, and vice versa. Hence we can conclude, from the limits on k above, that this example falls into the region where (1) three-wave parametric decay via ion sound is kinematically forbidden and (2) the WKB approximation is not valid, consistent with mode mixing.

5. Observations: January 19, 1998

There was a series of type III bursts beginning at 2000 UT on January 19, 1998, as seen by the radio part of the Waves experiment. The largest at low frequencies, and the one which seems to have given rise to Langmuir waves, was at about 2100 UT. The first Langmuir waves captured and telemetered by the TDS were at 2242 UT, although the TNR shows that the first Langmuir waves were at 2210 UT. A total of 15 events were captured over the period 2242–2324 UT. During this period the solar wind velocity was 380 km s^{-1}, and the electron temperature, both from the 3D Plasma experiment [*Lin et al.*, 1995], was 15 eV.

In contrast to the narrow spectra of the event of November 4 above, the spectra of the events of January 19 often showed two peaks with a wide separation, of the order of 700–1000 Hz. In Figure 8 we show the waveforms and a Fourier analysis from one of the events. The rapid modulation shows already that the frequency splitting must be of the order of 1 kHz, and the Fourier spectrum confirms this. One of the peaks in the spectrum has appreciable width, which makes an analysis into two waves suspect. In fact, however, the waves are changing rapidly. In Figure 9 we show the two-wave analysis for two short sections of the event. The left diagram is an analysis of the data between 6.0 and 7.5 ms, and the right diagram is of the data between 9.0 and 10.5 ms. As splitting is large, indicating that the primary must lie well above the plasma frequency, it is unlikely that these waves have an electromagnetic component. Nevertheless, what is shown is the analysis into electromagnetic waves, first because the waves are shown more clearly and second to demonstrate roughly the size of the errors in the electromagnetic fit. It will be seen that the trans-

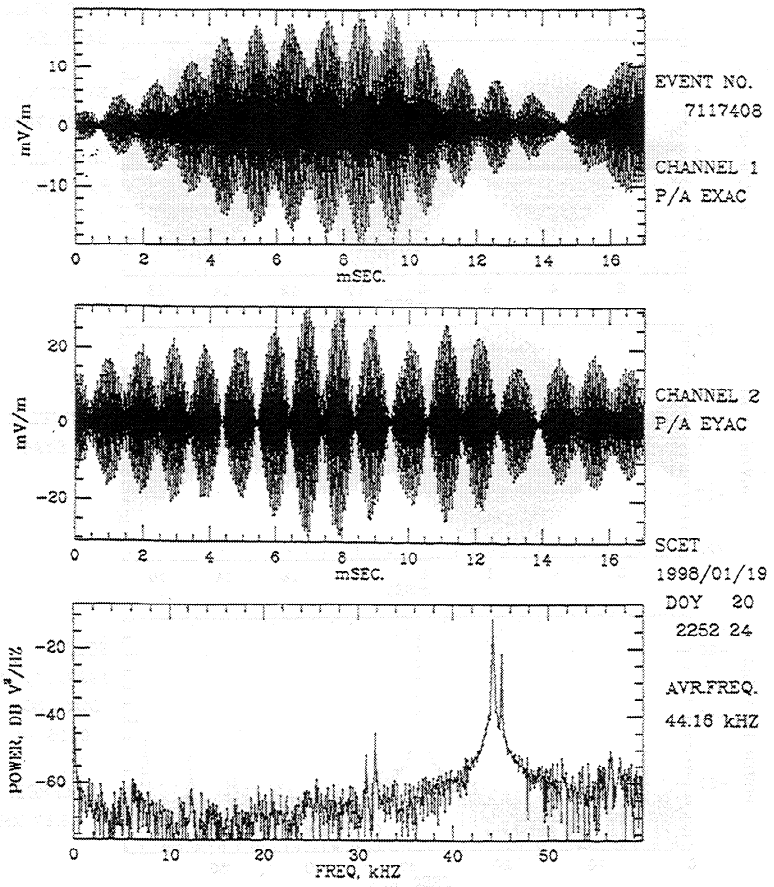

Figure 8. The waveforms of one of the events of January 19, 1998.

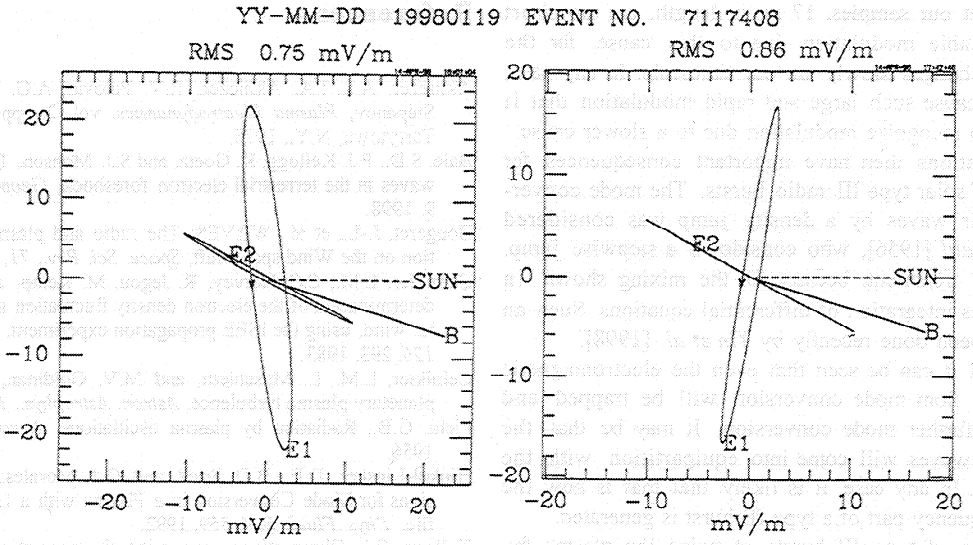

Figure 9. Analysis of the data of Figure 8 into two waves including data between (left) 6.0 and 7.5 ms and (right) 9.0 and 10.5 ms. In this case, only the results of the electromagnetic analysis are shown, but it is believed that the waves are electrostatic.

verse components are all smaller than those of Figures 5 and 6, which together with the considerable improvement in residuals in Figure 6 supports the identification of a real transverse component in Figure 6 at least. It will be seen that each diagram of Figure 9 shows a component aligned closely to the magnetic field and another component which has changed directions between the two diagrams. The component aligned with the magnetic field has the higher frequency in the spacecraft frame, which must also be the higher frequency in the solar wind frame, if one makes the reasonable assumption that the aligned component is a primary wave. One interpretation of this event is that the primary, generated with its k vector close to B by an electron beam, is decaying into other waves. During the first part of the event it decays into the daughter wave shown, but then a new daughter in a slightly different direction takes its place. The analysis for the time period between the two shown makes a poor fit, presumably because of the presence of three waves.

If it is assumed that the primary remains reasonably constant in frequency and wave vector, then making the assumption than the observed difference frequency of the daughter waves is mainly due to Doppler shift, we can write, taking into account the angles with the solar wind and assuming that the wave E2 is in the more backward of the two possible choices,

$$\Delta\omega = \left(k_1 \cos 23° + k_2 \cos 102°\right) v_{sw} \tag{14}$$

The observed splitting is .99 kHz. Together with the solar wind speed above, this gives limiting values of the wave vector of

$$\begin{aligned} \frac{k_1 c}{\omega_p} &= 19 \quad k_2 = 0 \\ \frac{k_1 c}{\omega_p} &= 24 \quad k_1 = k_2 \end{aligned} \tag{15}$$

These are, obviously, consistent with our initial assumption that these waves are electrostatic. From the list of values in section 2 it can be seen that this event corresponds to the usual treatment of Langmuir wave decay: The WKB approximation holds, etc., three-wave parametric decay is allowed, and we suggest that the secondary wave, E1 in Figures 8 and 9, is the daughter in such a decay.

6. Discussion and Summary

We have analyzed, in terms of two waves of different observed frequencies and different directions, two sets of waves from "local" type III solar radio bursts, i.e., those accompanied by Langmuir waves, chosen because of their different bandwidths. The Langmuir waves of a type III burst on November 4, 1997, show the characteristics expected for small wave number k as if they were generated by a high-energy beam and therefore lie very close to the plasma frequency. The frequency spread is small even for pairs of waves at widely different angles. As the Doppler shift sets a minimum frequency spread of the order of $\Delta k v_{sw}$, the wave number must be small. There is little sign of parametric decay or other nonlinear processes, and their wave number is probably below the limit of three-wave parametric decay via ion sound waves. The waves seem to be bouncing around between reflecting surfaces and show some evidence of transverse components, which may be interpreted as evidence for mode mixing and consequent linear mode conversion.

The Langmuir waves of the burst on January 19, 1998, are considerably different. Many of the spectra show peaks separated by frequencies up to 1 kHz and show the characteristics expected for waves of larger wave number.

Of the five possible causes of modulation suggested in section 3, we have shown evidence for three, namely, reflection, instability, and decay. We have chosen not to discuss examples of the first of the causes in section 3, modulation due to a narrow distribution of wave vectors in k space, but in fact, a large number of cases probably fall into that category. We have not found cases where the modulation is demonstrably due to changes in plasma parameters, and on the basis of Figure 1, we

would expect that our samples, 17 ms in length, are too short to show appreciable modulation due to this cause, for the plasma density changes slowly on our timescale. In any case, the other effects cause such large and rapid modulation that it would be hard to recognize modulation due to a slower cause.

These observations then have important consequences for the generation of solar type III radio bursts. The mode conversion of Langmuir waves by a density jump was considered very early by *Field* [1956], who considered a stepwise jump. A more realistic treatment, because of the mixing shown in Figure 2, requires integration of differential equations. Such an integration has been done recently by *Yin et al.* [1998].

From Figure 1 it can be seen that even the electromagnetic waves resulting from mode conversion will be trapped and scattered, with further mode conversion. It may be that the electromagnetic waves will come into equipartition with the Langmuir waves. In any case, it is likely that that is how the fundamental frequency part of a type III burst is generated.

The generation of type III bursts at twice the plasma frequency has, from the first theoretical efforts, required two Langmuir waves with wave vectors in nearly opposite directions. Various efforts have been made to understand the generation of the opposed wave, but as pointed out by *Kellogg* [1986], it is a simple consequence of the expected level of density fluctuations and the reflection implied. However, it has always been assumed that the two waves must be almost exactly opposite, because it is assumed that the wave number of the $2f_p$ electromagnetic waves is very small compared to the Langmuir waves, so that their wave numbers must add nearly to zero. However, this is no longer true in the region of Figure 2 (right), where the Langmuir wave numbers are also small. Hence two Langmuir waves of somewhat different directions may be added in this region to give a $2f_p$ electromagnetic wave, thus improving the efficiency of the process as well as providing large numbers of such pairs. We have shown some events which can most easily be interpreted as reflection, to confirm this suggestion.

Acknowledgments. This work was supported by the National Aeronautics and Space Administration grants NAG5-2838 and NAG5-2815. Paul J. Kellogg would like to thank Robert Manning, J.-L. Bougeret, and J.-L. Steinberg for their hospitality at the Observatoire de Paris-Meudon.

Janet G. Luhmann thanks Reinhard Schlickeiser and another referee for their assistance in evaluating this paper.

References

Akhiezer, A.I., I.A. Akhiezer, R.V. Polovin, A.G. Sitenko, and K.N. Stepanov, *Plasma Electrodynamics*, vol. 2., pp. 94ff, Pergamon, Tarrytown, N.Y., 1975.

Bale, S.D., P.J. Kellogg, K. Goetz, and S.J. Monson, Transverse Z-mode waves in the terrestrial electron foreshock, *Geophys. Res. Lett., 25*, 9, 1998.

Bougeret, J.-L., et al., WAVES: The radio and plasma wave investigation on the Wind spacecraft, *Space. Sci. Rev., 71*, 231, 1995.

Celnikier, L.M., C.C. Harvey, R. Jegou, M. Kemp, and P. Moricet, A determination of the electron density fluctuation spectrum in the solar wind, using the ISEE propagation experiment, *Astron. Astrophys., 126*, 293, 1983.

Celnikier, L.M., L. Muschietti, and M.V. Goldman, Aspects of interplanetary plasma turbulence, *Astron. Astrophys., 181*, 138, 1987.

Field, G.B., Radiation by plasma oscillations, *Astrophys.J., 124*, 555, 1956.

Hinkel-Lipsker, D.E., B.D. Fried, and G.J. Morales, Analytic Expressions for Mode Conversion in a Plasma with a Linear Density Profile, *Phys .Fluids B, 4*, 559, 1992.

Kellogg, P.J., Observations concerning the generation and propagation of type III solar bursts, *Astron. Astrophys., 169*, 329, 1986.

Kellogg, P.J., and N. Lin, Ion isotropy and fluctuations in the solar wind, paper presented at 31st ESLAB Symposium: Correlated phenomena at the Sun, the Heliosphere and in Geospace, *SP-415*, Eur. Space Res. and Technol. Cent., Noordwijk, Netherlands, 1997.

Kraus-Varban, D., Beam instability of the Z mode in the solar wind, *J. Geophys. Res., 94*, 3527, 1989.

Lin, R.P., et al., A three-dimensional plasma and energetic particle investigation for the WIND spacecraft, *Space Sci. Rev., 71*, 125, 1995.

Neugebauer, M., The enhancement of solar wind fluctuations at the proton thermal gyroradius, *J. Geophys. Res., 80*, 998, 1975.

Neugebauer, M., Corrections to and comments on the paper 'The enhancement of solar wind fluctuations at the proton thermal gyroradius,' *J. Geophys. Res., 81*, 2447, 1976.

Unti, T.W.J., M. Neugebauer, and B.E. Goldstein, Direct measurement of solar wind fluctuations between 0.0048 and 13.3 Hz, *Astrophys.J., 180*, 591, 1973.

Yin, L., M. Ashour-Abdalla, M. El-Alaoui, J.M. Bosqued, and J.-L. Bougeret, Generation of electromagnetic f_{pe} and 2 f_pe waves in the Earth's electron foreshock via linear mode conversion, *Geophys. Res. Lett., 25*, 2609, 1998.

S. D. Bale, Space Sciences Laboratory, University of California, Berkeley, CA 94720.

K. Goetz, P.J. Kellogg, and S.J. Monson, School of Physics and Astronomy, 116 Church Street, SE, Minneapolis, MN 55455-0112. (kellogg@waves.space.umn.edu)

(Received August 10, 1998; revised January 11, 1999;
accepted March 23, 1999.)